https://doi.org/10.5194/amt-2023-96
Preprint. Discussion started: 11 May 2023
© Author(s) 2023. CC BY 4.0 License.

Atmospheric Measurement Techniques Discussions

Revision of an open-split-based dual inlet system for elemental and isotope ratio mass spectrometers with a focus on clumped isotope measurements

Stephan Räss [1,2], Peter Nyfeler [1,2], Paul Wheeler [3], Will Price [3], and Markus Christian Leuenberger [1,2]

[1]Climate and Environmental Physics, University of Bern, Bern, Switzerland
[2]Oeschger Centre for Climate Change Research, University of Bern, Bern, Switzerland
[3]Elementar UK Ltd., Isoprime House, Earl Road, Cheadle Hulme, Stockport - SK8 6PT, United Kingdom

Correspondence: Stephan Räss (stephan.raess@unibe.ch)

Abstract. In this work we present a revision of an open-split-based dual inlet system for elemental and isotope ratio mass spectrometers (IRMS), which was developed by the Climate and Environmental Physics Division of the University of Bern two decades ago. Besides discussing the corresponding improvements we show that with this inlet system (NIS-II) external precisions can be achieved that are high enough to perform measurements of multiply-substituted isotopologues (clumped isotopes) on pure gases. For the clumped isotope ratios 35/32 and 36/32 of oxygen we achieved standard deviations of $3.4 \cdot 10^{-9}$ and $4.9 \cdot 10^{-9}$, respectively, that we calculated from 60 interval means (20 s integration) of pure oxygen gas measurements.

Moreover, we report various performance tests and show that with the NIS-II delta values of various air components can be measured with precisions of order tenths of per meg and higher. In addition, we demonstrate that our new open-split-based dual inlet system allows to measure some of these delta values with significantly higher precisions than a NIS-I (precursor of NIS-II) and a conventional changeover-valve-based dual inlet system (tests performed with an Elementar iso DUAL INLET). The greatest discrepancies between the NIS-II and the iso DUAL INLET were observed for $\delta_{32/28}$ and $\delta_{44/28}$; the differences in the external precisions were 4 $\mathrm{per\,meg}$ and 35 $\mathrm{per\,meg}$ (10 SA/STD measurements), respectively. With respect to the reproducibility of $\delta_{32/28}$ means, the deviations from a reference value were even larger, namely around 0.1 ‰.

Due to the successful preliminary tests regarding measurements of clumped isotope ratios, we will continue our work in this area to perform clumped isotope studies according to common practices.

1 Introduction

Most isotope ratio mass spectrometers (IRMS) are fed by means of a changeover-valve-based dual inlet system. While the external precision of such a system is of the order hundredths of per mil (Leuenberger, 2000) and thus high enough for many common applications, it is too low for measurements requiring a very high precision; for example, the annual variability of $\delta_{\mathrm{O_2/N_2}}$ measured on ambient air is of the order tenths of per meg (Keeling, 2021). In order to make measurements like these possible, more than 20 years ago, the Climate and Environmental Physics Division of the University of Bern developed an open-split-based dual inlet system whose basic principle was adapted from gas chromatography/mass spectrometry (GC/MS)

https://doi.org/10.5194/amt-2023-96
Preprint. Discussion started: 11 May 2023
© Author(s) 2023. CC BY 4.0 License.

Atmospheric Measurement Techniques Discussions

open splits (Brand, 1995).

Basically, changeover-valve-based dual inlet systems consist of two individual metal bellows (one for storing the sample gas and the other for the standard gas), two separate gas lines and a changeover valve block. The metal bellows, which typically have a volume between 20 ml and 100 ml (Leuenberger, 2000), are compressible such that the signals of the two gases can be equalised. During operation, the gases are transported from the two bellows to the changeover valve block; there, the gas is selected that is admitted to the mass spectrometer. By switching between the two gases the isotope ratios and the corresponding delta values can be determined. In order to guarantee a similar gas consumption for both sides of the inlet system, the gas that is not admitted to the mass spectrometer is consumed by one of the inlet system's pumps.

Unfortunately, these changeover-valve-based dual inlet systems have some drawbacks that deteriorate the measurement precision; firstly, as the gas flux through such inlet systems is not continuous and many metallic surfaces are present, surface adsorption/desorption effects on these surfaces may occur (Leuenberger, 2015). This can in turn lead to variations in the gas composition. Secondly, isotope fractionation (Leuenberger, 2000) may occur because the pressure of the gases under study are altered by means of the inlet system's valves.

As reported by Leuenberger (2000), these issues can be overcome by means of an open-split-based dual inlet system. In fact, the primary goals of Leuenberger (2000) were to improve the pressure and temperature adjustment, to reduce adsorption/desorption effects on metallic surfaces and to build an inlet system that is as symmetrical as possible. In order to reduce signal variations to 0.25 ‰, the pressure and the temperature may not vary more than 0.1 mbar and 0.03 $^{\circ}\mathrm{C}$, respectively (Leuenberger, 2000). Due to these requirements the gas flow rates of the measured gases must be highly constant, otherwise non-linearity effects may lead to fractionations noticeable on the per meg scale (Leuenberger, 2000). The three aims were achieved as follows (Leuenberger, 2000): The changeover valve block was replaced by a Y-shaped open split interface, which was situated inside of an aluminum container. The temperature of the container could be regulated by means of cartridge heaters and for the pressure regulation a vacuum pump as well as a pressure controller were used. By means of this design, it was possible to fully separate the inlet system from the ion source. For the transfer of gas from the gas containers to the open split and from the open split to the mass spectrometer glass capillaries were used.

The dual inlet system we present in this paper, the „New Inlet System II“ (NIS-II), is the successor of the first version (NIS-I) described in the paper by Leuenberger (2000). In addition to high precision measurements of conventional elemental and isotope ratios, the NIS-II was built to detect multiply-substituted isotopologues (clumped isotopes). For clumped isotope studies, the corresponding isotope ratios usually need to be measured with precisions of the order 10^{-5} to 10^{-6} (Eiler, 2007).

In general, the basic working and design principles of both versions of the NIS are identical. However, the NIS-I had two major disadvantages we now eliminated:

- Due to the fact that the open split interface was implemented by means of a Y-shaped piece of glass (two inlets for the transport of standard or sample gas into the open split and one for the gas transfer to the IRMS) it was difficult to purge

https://doi.org/10.5194/amt-2023-96
Preprint. Discussion started: 11 May 2023
© Author(s) 2023. CC BY 4.0 License.

Atmospheric Measurement Techniques Discussions

the open split thoroughly. In order to attain good results, the glass capillaries had to be equipped with rubber seals at their ends and had to be positioned very precisely. Not only did the proper positioning of the rubber seals require many attempts, but also position checks were necessary on a regular basis.

- The second drawback concerns the mechanism responsible for switching between the sample (SA) and the standard (STD) gas. This mechanism was based on two pneumatic pistons, which were put in motion by means of two electromagnetic valves. Although this mechanism did not have a noticeable influence on the measurement results it was not ideal; in order to ensure a gas-tightness over five decades of pressure, the pneumatic valves had to be equipped with two-step seals that required frequent maintenance.

In what follows, we first describe the design and working principles of the NIS-II. Thereafter we report the results of different studies we carried out to assess the performance of the new inlet system. Moreover we present a comparison of our new inlet system to its precursor as well as to a common changeover-valve-based dual inlet system (Elementar iso DUAL INLET). The central part of the paper, the feasibility study of clumped isotope measurements on air components, is documented at the end.

2 Dual inlet system revision

2.1 Design principle

The housing of our new dual inlet system, the NIS-II, consists of a cylindrical aluminum frame with an inner diameter of 31 cm and a wall thickness of 2 cm. The housing, whose height is 11 cm, can be closed with a cap made of acrylic glass having a thickness of 2 cm. This cap can in turn be fixed to the aluminum frame by means of 16 screws. Next to the corresponding screw holes there is a circular recess for a rubber seal that improves the gas tightness of the container (see Fig. 1).

In the centre of the container we installed an aluminum base plate on which different components are mounted: On the top end of the base plate there is a glass tube acting as an open split interface. This tube is closed at its back end and has a length of approximately 4 cm. This glass tube, which has an inner diameter of 1.4 mm, is fixed to the base plate by means of an intermediate piece of aluminum, which allows to insert the open split in a horizontal position. While the intermediate piece of aluminum is screwed down on the base plate, the glass tube can be removed easily as the fixation to the intermediate piece is realised by means of tape. On the lower end of the container's base plate there are two Blue Bird Standard BMS-660 servos, which together constitute the centrepiece of the dual inlet system's switching mechanism. These servos can be controlled by means of an Olimex PIC-P18 development board (outside of the container) and the mass spectrometer's software (Elementar isoprime precisION running ionOS). In contrast to the pneumatic valves of the NIS-I, the servos require little maintenance and do not influence the temperature inside of the container significantly. Each of the servos' arms is in turn attached to a brass plate that can be moved along 8 cm long rails. On each of these moveable brass plates we installed a 1/16 in Swagelok bulkhead union that is used for the fixation of a gas transfer capillary. In order to fix the capillary, we first remove the union's nuts, guide the capillary through the union, add a BGB Analytik graphite/vespel 1/16 $\mathrm{in} \times 0.4\ \mathrm{mm}$ ferrule and then mount the nuts again.

https://doi.org/10.5194/amt-2023-96
Preprint. Discussion started: 11 May 2023
© Author(s) 2023. CC BY 4.0 License.

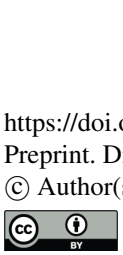

Atmospheric Measurement Techniques Discussions

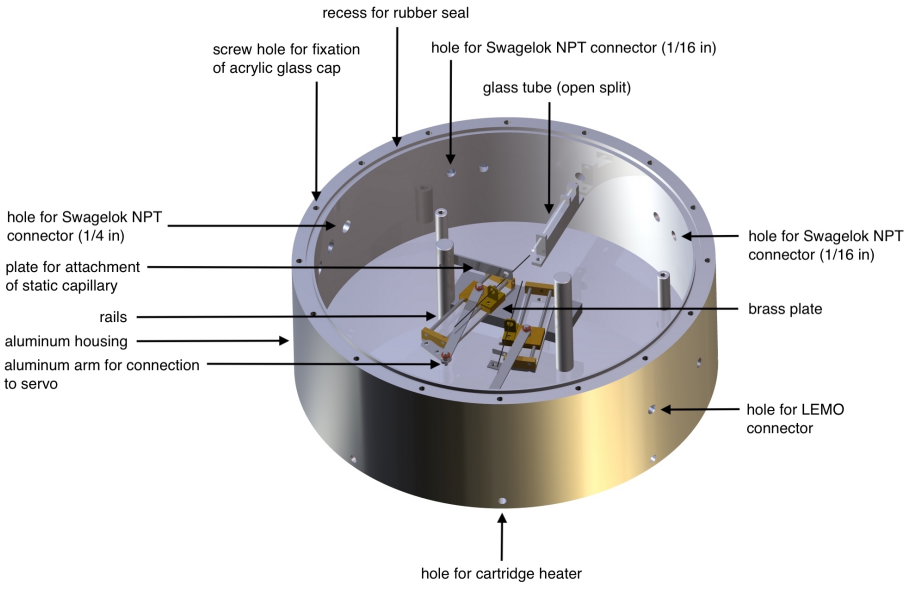

Figure 1. Computer aided design (CAD) image of the NIS-II container created by the mechanical workshop team of the Climate and Environmental Physics Division of the University of Bern with annotations added by the authors.

As pointed out before, the gas transfer is realised by means of glass capillaries. For this transfer at least three capillaries are required: One capillary is static and connects the open split to the IRMS. The other two capillaries, which are fixed to the moveable brass plates, transfer gas from the sample and standard gas containers, respectively, to the open split. Please note that the static capillary is installed in a similar way as the other two, except that the capillary holder is not mounted on a moveable brass plate but on a static piece of aluminum near the centre of the base plate.

For guiding the capillaries into the container, we integrated five Swagelok NPT connectors (1/16 in) into the container walls. Of these five connectors at least three are used, namely one per capillary. For the fixation of the capillaries the same principle was applied that was used for the capillary holders mounted on the moveable brass plates.

In addition to these five connectors we added three larger Swagelok NPT ports (1/4 in). One of these ports is used for connecting an ANALYT-MTC pressure controller to the inlet system that, along with a KNF N920 (KT.29.18G) feed pump, stabilises the pressure inside of the container. For most applications, the pressure inside of the container is set to a value between 20 mbar and 250 mbar; in fact, this eventually depends on the capillaries and the desired signal height. The second of these three ports is connected to a pure argon gas cylinder, which is used for the purging of the container; typically, the flow rate of this gas is held constant at a value between 5 $\mathrm{ml\,min^{-1}}$ and 10 $\mathrm{ml\,min^{-1}}$. Between the container and the pressure controller as well as between the container and the gas cylinder there are Nupro Gas Shut-Off Valves, which can be used to isolate the container from the laboratory. In addition to the gas ports we embedded three LEMO connectors in the container walls which are used for the signal transmission and the power supply of the electronic components situated on the inside of the container.

https://doi.org/10.5194/amt-2023-96
Preprint. Discussion started: 11 May 2023
© Author(s) 2023. CC BY 4.0 License.

Atmospheric Measurement Techniques Discussions

In order to regulate and stabilise the temperature of the NIS-II container, we use electric cartridge heaters. For the placement of these heaters, we drilled eight equally distributed holes into the bottom end of the container walls. Moreover, for the fixation of the heaters with screws, eight holes were drilled into the bottom of the container. In order to improve the heat transmission, we dipped the cartridge heaters into a heat sink compound before introducing them into the holes. The heating status of the container can be monitored by means of an external temperature control unit, which responds to a Pt100 temperature sensor located on the inside of the NIS-II container below the aluminum base plate. To reduce the occurence of thermal fractionation the set temperature should be similar to the temperature of the mass spectrometer.

2.2 Working principle

The NIS-II is built in such a way that there is an uninterrupted gas flow through all of the capillaries. During operation, one of the two moveable capillaries is situated inside of the open split while the other is kept outside; while the gas of the former capillary is automatically transferred to the static capillary, which is also situated inside of the open split, the gas of the other capillary is poured into the free space of the NIS-II container. As the static capillary is connected to the mass spectrometer, the gas eventually reaches the ion source. During this procedure, the NIS-II container is constantly flushed with a purge gas and is held at a constant pressure.

When switching between the moveable capillaries, the system goes through the following steps: At the end of each measuring interval the capillary that is currently outside of the open split is inserted into it and subsequently the other one is retracted. By fully inserting the former capillary into the glass tube before the latter is pulled out, we ensure that the open split remains sealed off from the container atmosphere. However, as this type of sealing also relies on a gas flow rate that is high enough to prevent container gas from entering the open split, we had to find a way to detect possible leaks. This can for example be achieved by selecting a container purge gas that the mass spectrometer's Faraday collector array can detect. For the studies presented in this work we used pure argon (stored in regular steel cylinder).

The fundamental principle that is applied to transfer gas from the two gas sources to the mass spectrometer is the generation of flow by means of a pressure gradient. In order to provide a continuous gas flow, the pressure has to gradually decrease from the gas sources to the mass spectrometer.

The gas flow rate through a capillary, which depends on the pressure gradient as well as on the length and the inner diameter of the capillary, can be estimated by means of the Hagen-Poiseuille equation

$$\frac{dV}{dt} = -\frac{\pi r^4}{8\eta} \cdot \frac{\Delta p}{l}. \tag{1}$$

In Eq. (1), dV/dt denotes the volumetric flow rate, η the dynamic viscosity of the fluid, r and l the inner radius and the length of the capillary, respectively, and Δp the pressure difference between the two ends of the capillary.

https://doi.org/10.5194/amt-2023-96
Preprint. Discussion started: 11 May 2023
© Author(s) 2023. CC BY 4.0 License.

Atmospheric Measurement Techniques Discussions

While changeover-valve-based dual inlet systems need to adjust the gas pressure to compensate the gas loss, namely by means of bellow compression, this is not necessary for our system; throughout the entire gas transfer from the gas sources via the NIS-II to the mass spectrometer the gases are subjected to the same pressure conditions. If one would like to alter the pressure inside of the system, this can be achieved with the help of the ANALYT-MTC pressure controller and the KNF N920 feed pump. This pressure regulation in turn allows to alter the gas flow into the ion source and therefore the signal intensity.

3 Results and discussions

For the studies presented in this section, we either measured gas cylinders containing compressed air or pure oxygen from Carbagas, Switzerland. In the following, when referring to gas cylinders we will use the prefix „LUX“ for aluminum Luxfer cylinders and „SC“ for regular steel cylinders. Typically, for the air measurements we used gas from the cylinders LUX 3588 and LUX 3591. For oxygen measurements the cylinders SC 84567 ($O_2 \geq 99.998$ %), SC 62349 ($O_2 \geq 99.9995$ %) and SC 540546 ($O_2 \geq 99.9995$ %) were available.

Our main measurement setup, which was set up according to the descriptions in Sect. 2, consists of the Elementar isoprime precisION IRMS and the open-split-based NIS-II. For comparison purposes, we also used the changeover-valve-based Elementar iso DUAL INLET for certain experiments. Our isoprime precisION is equipped with a Faraday collector array for measuring air components. This array consists of 10 cups designed for measuring the mass-to-charge (m/z) ratios 28 $\mathrm{u\,e^{-1}}$ to 30 $\mathrm{u\,e^{-1}}$, 32 $\mathrm{u\,e^{-1}}$ to 36 $\mathrm{u\,e^{-1}}$ as well as 40 $\mathrm{u\,e^{-1}}$ and 44 $\mathrm{u\,e^{-1}}$. Hereafter, we will drop the units of mass-to-charge ratios for the sake of simplicity. The delta values we present in this section were calculated from the measurement signals as described in Appendix A. The notation we adopted for delta values referring to the isotope ratio R is δ_R.

The measurements we carried out with the Elementar isoprime precisION were composed of six sample gas measuring intervals and six or seven standard gas intervals; these intervals were executed in alternating order. In the following, measurements of this type will be denoted as „SA/STD measurements“. The integration time of each of the measuring intervals was set to 20 s. Unless otherwise stated, external precisions derived from such measurement series were always assessed by calculating the standard deviation of the mean delta values (or isotope ratios) of the individual measurements. For the assessment of the internal precision of delta values (or isotope ratios) we computed the mean value of the standard errors of the individual measurements.

The first performance test we carried out concerned the purging of the new open split. Thereafter, we studied the measurement precision limits and the signal stability of the new measurement setup. As a next step, we determined the precisions with which delta values of air components can be measured and compared these results to those obtained with the NIS-I and the iso DUAL INLET. As a last step, we used the NIS-II to measure air and pure oxygen in order to assess the feasibility of clumped isotope measurements with our setup.

https://doi.org/10.5194/amt-2023-96
Preprint. Discussion started: 11 May 2023
© Author(s) 2023. CC BY 4.0 License.

Atmospheric Measurement Techniques Discussions

In the following subsections, we first report our experience with the new inlet system's maintenance and then discuss the previously mentioned studies along with their results.

3.1 Maintenance

With regard to the maintenance of the NIS-II we clearly saw an improvement when compared to the first version of the inlet system; within one year of almost daily use the only maintenance required was the removal of dust from the rails of the capillary switching mechanism. This dust, which mainly accumulates due to mechanical abrasion, had to be removed twice in this period of time. After cleaning the rails with alcohol, they have to be greased with an oil having a low vapour pressure. When including the time needed to open and close the NIS-II container, this procedure takes approximately 30 min. When the NIS-II is operated over longer periods of time, at some point, the servos driving the capillary switching mechanism have to be replaced. This is usually the case after 1 to 2 years. Nevertheless, when the NIS-II is heavily used or the servos are of poor quality, this replacement might also be due sooner.

3.2 Open split purging

As the open split interface is not mechanically sealed off from the dual inlet system's container atmosphere this has to be ensured by establishing a gas flow rate that is high enough to prevent container gas from reaching the ion source. In the following, this gas flow rate will be referred to as „purge flow rate". This flow rate must not be confused with the flow rate of the container purging gas (argon).

In order to study the influence of the purge flow rate on the measurement signals, we connected the pure oxygen gas cylinder SC 84567 to the standard inlet of the NIS-II and performed 12 time scans (Faraday cup signal recording at a fixed acceleration voltage) at different volumetric purge flow rates. In order to vary this flow rate we introduced an ANALYT-MTC mass flow controller (MFC) of the 358 series between the gas cylinder and the NIS-II. As the pressure inside of the NIS-II container was kept constant, namely at $(20 \pm 1)\ \mathrm{mbar}$, the pressure variation by means of the MFC allowed to alter the volumetric purge flow rate.

In Fig. 2, the mean signal of the $m/z = 40$ cup recorded during the aforementioned time scans is shown as a function of the measured volumetric flow rate, namely in cubic centimetres per minute (measured) as well as in standard cubic centimetres per minute (calculated). We performed the standardisation with respect to pressure (101325 Pa) and temperature (273.15 K). For the calculations we used the ideal gas law as well as the temperature and the pressure readings of the MFC. As an aside, it may be mentioned that the relevant pressure is not the pressure reading of the MFC but the mean value of the pressure reading and the NIS-II container pressure (20 mbar); the reason for this is that according to Eq. (1) the pressure between the MFC and the NIS-II container decreases linearly.

The data shown in Fig. 2 indicate potential contaminations of pure oxygen with gas of the NIS-II container atmosphere. This gas is mainly composed of the purge gas argon and the analyte. Additionally, as the LEMO connectors of the container are only gas tight to a certain degree, at pressures distinctly below atmospheric pressure, it cannot be excluded that also small

https://doi.org/10.5194/amt-2023-96
Preprint. Discussion started: 11 May 2023
© Author(s) 2023. CC BY 4.0 License.

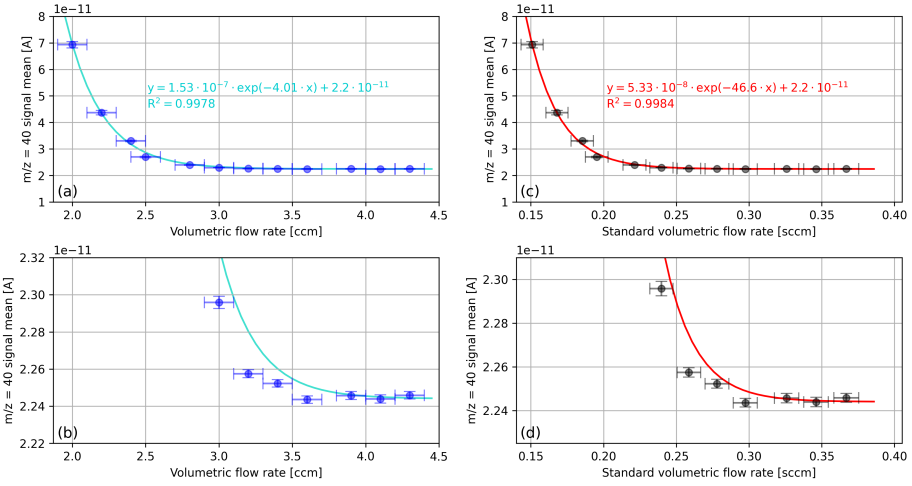

Figure 2. Mean $m/z = 40$ cup signals recorded during a series of 3 min oxygen time scans corresponding to different volumetric flow rates. (a) Signals of $m/z = 40$ cup as a function of the measured volumetric flow rate in cubic centimetres per minute. (c) Same data as in (a) but in standard cubic centimetres per minute (mass flow). (b) Zoomed-in view of (a) and (d) zoomed-in view of (c). The vertical error bars correspond to the standard deviations of the $m/z = 40$ signal. In panel (a), the horizontal error bars indicate the approximate fluctuation of the flow rate reading (0.1 sccm) and in panel (b) this error was converted to standard cubic centimetres per minute.

amounts of laboratory air are present in the container atmosphere.

As can be seen from Fig. 2, the $m/z = 40$ signal decreases exponentially and levels out around (3.9 ± 0.1) ccm, which corresponds to (0.33 ± 0.01) sccm. Due to the fact that the NIS-II container was primarily filled with argon it can be concluded that for purge flow rates exceeding 0.33 sccm the open split is isolated from the container atmosphere to a satisfactory degree; this minimum purge flow rate is slightly higher than the 0.16 sccm (120 nmol s^{-1}) (Leuenberger, 2000) that were required for the purging of the Y-shaped open split of the NIS-I. Furthermore, the sample consumption of our open-split-based dual inlet systems is higher than that of a changeover-valve-based dual inlet system, namely due to the purging of the open split. The gas consumption depends on the volume and design of the open split.

Although the minimum purge flow rate of the straight open split is slightly higher than that of its Y-shaped precursor, we consider it a major improvement; during operation the new open split causes no noteworthy problems. Apart from that, it is easy to install, replace and manufacture.

3.3 Measurement precision limits

The measurement precision that can be attained with an IRMS and its inlet system is limited by different factors. In this subsection, we discuss the system noise and the errors associated with counting statistics because those are closely linked with

https://doi.org/10.5194/amt-2023-96
Preprint. Discussion started: 11 May 2023
© Author(s) 2023. CC BY 4.0 License.

Atmospheric Measurement Techniques Discussions

Table 1. Faraday cup signal means determined with an Elementar isoprime precisION in the absence of gas (collector zeros) as well as in the presence of air (LUX 3588 admitted with the NIS-II). For the electronic zeros the acceleration voltage was turned off. The mean values were calculated from each of the 5 min measurements without removing any data points and without applying any corrections. For the uncertainties of the cup signals the standard deviations of the cup signals were computed. In the first column of the table, the mass-to-charge ratios of the 10 Faraday cups are indicated.

Cup	Collector zeros [A]	Electronic noise [A]	Air [A]
28	$1.0023 \cdot 10^{-9} \pm 6 \cdot 10^{-13}$	$1.0019 \cdot 10^{-9} \pm 5 \cdot 10^{-13}$	$2.920 \cdot 10^{-8} \pm 3 \cdot 10^{-11}$
29	$1.0029 \cdot 10^{-11} \pm 3 \cdot 10^{-15}$	$1.0016 \cdot 10^{-11} \pm 3 \cdot 10^{-15}$	$2.145 \cdot 10^{-10} \pm 2 \cdot 10^{-13}$
30	$1.0029 \cdot 10^{-11} \pm 3 \cdot 10^{-15}$	$1.0022 \cdot 10^{-11} \pm 3 \cdot 10^{-15}$	$4.599 \cdot 10^{-11} \pm 3 \cdot 10^{-14}$
32	$1.0039 \cdot 10^{-9} \pm 4 \cdot 10^{-13}$	$1.0034 \cdot 10^{-9} \pm 4 \cdot 10^{-13}$	$7.719 \cdot 10^{-9} \pm 7 \cdot 10^{-12}$
33	$1.0080 \cdot 10^{-11} \pm 3 \cdot 10^{-15}$	$1.0075 \cdot 10^{-11} \pm 3 \cdot 10^{-15}$	$1.4797 \cdot 10^{-11} \pm 6 \cdot 10^{-15}$
34	$1.0031 \cdot 10^{-11} \pm 4 \cdot 10^{-15}$	$1.0026 \cdot 10^{-11} \pm 3 \cdot 10^{-15}$	$3.410 \cdot 10^{-11} \pm 3 \cdot 10^{-14}$
35	$1.0002 \cdot 10^{-11} \pm 3 \cdot 10^{-15}$	$1.0001 \cdot 10^{-11} \pm 3 \cdot 10^{-15}$	$9.507 \cdot 10^{-12} \pm 3 \cdot 10^{-15}$
36	$1.0045 \cdot 10^{-11} \pm 2 \cdot 10^{-15}$	$1.0041 \cdot 10^{-11} \pm 2 \cdot 10^{-15}$	$9.928 \cdot 10^{-12} \pm 3 \cdot 10^{-15}$
40	$1.0020 \cdot 10^{-11} \pm 4 \cdot 10^{-15}$	$9.987 \cdot 10^{-12} \pm 3 \cdot 10^{-15}$	$5.689 \cdot 10^{-10} \pm 6 \cdot 10^{-13}$
44	$1.0062 \cdot 10^{-9} \pm 2 \cdot 10^{-13}$	$1.0061 \cdot 10^{-9} \pm 3 \cdot 10^{-13}$	$1.0310 \cdot 10^{-9} \pm 2 \cdot 10^{-13}$

the measurement setup itself. Nonetheless, it is important to be aware of the fact that there also exist external factors such as sample purity and sample handling that have an influence on the measurement precision as well.

3.3.1 System noise

In order to assess the system noise of the Elementar isoprime precisION we took the following approaches:

- We closed the mass spectrometer's main gas admission valve, evacuated the mass spectrometer and then recorded the Faraday collector signals during 5 min. In the following, we will refer to these measurement signals as „collector zeros".
- We turned off the acceleration voltage (AV) and then recorded the cup signals for 5 min while admitting air to the mass spectrometer by means of the NIS-II. We will refer to the corresponding data as „electronic noise".

In Table 1, the outcomes of the measurements outlined before are shown. In addition, in order to get a first impression on the measurement precision of regular measurements, we also performed a 5 min time scan of compressed air at an acceleration voltage around 4461 V. The results of this measurement, which were derived from the raw data (no background corrections), are also shown in Table 1.

When comparing the collector zeros to the electronic noise shown in Table 1 it can be seen that they are almost identical. This is reasonable, because in neither case are ions reaching the cups; thus, signals are generated by system noise alone.

https://doi.org/10.5194/amt-2023-96
Preprint. Discussion started: 11 May 2023
© Author(s) 2023. CC BY 4.0 License.

Atmospheric Measurement Techniques Discussions

Furthermore, it stands out that the mean values of these noise indicators and the corresponding standard deviations are very similar for all of the cups, except for the dominant mass-to-charge ratios 28, 32 and 44; these are measured at low gain (10^9 Ω resistors) instead of high gain (10^{11} Ω resistors). The means and standard deviations of these three cup signals are around 2 orders of magnitude higher than the corresponding values of the remaining cups. Furthermore, from the standard deviations of the collector zeros and the electronic noise one learns that the cup signals with high and low gain can be recorded with maximum precisions of order $1 \cdot 10^{-15}$ A and $1 \cdot 10^{-13}$ A, respectively.

When comparing the collector zero measurement to the measurement of air it is noticeable that the standard deviations are very similar for the mass-to-charge ratios 33, 35, 36 and 44. In contrast, the standard deviations of the other cup signals are around 1 to 2 orders of magnitude higher for the air measurement; for instance, this can be caused by recombination and scrambling in the ion source or by statistical effects. Although we cannot rule out that the discrepancies were induced by the inlet system, this is rather unlikely since a deterioration of the standard deviation cannot be observed for all of the cup signals.

3.3.2 Counting statistics

As mentioned in the introduction of this subsection, among the limits of the system's measurement precision there is the so-called „shot noise limit", which is associated with counting statistics. Basically, this type of noise occurs because the number of ions generated by electron impact ionisation is not constant but approximately distributed according to the Poisson distribution. When denoting the number of ions as N, the standard deviation (or absolute error) of the Poisson distribution is given by $\sqrt{N}$ and the relative error by $\sqrt{N}/N$.

In panel (a) of Fig. 3, shot noise limits (relative error of Poisson distribution) and relative standard errors of Faraday cup signals are displayed. For the calculation of these values we used the first 60 s of the time scan of air summarised in Table 1; additionally, we computed the same standard errors for the collector zero data set of this table (in Fig. 3 denoted as „background"). From panel (a) of Fig. 3 it can be seen that the standard errors of the background are very close to the shot noise limit; this also holds true for some of the signals recorded during the time scan of air, namely for $m/z = 33$, $m/z = 35$, $m/z = 36$ and $m/z = 44$. Nevertheless, for the time scan of air, most of the standard errors are higher than the errors of the other two data sets. From this it can be concluded that, in general, effects other than counting statistics are limiting the measurement precision. This becomes even clearer when the same error calculations are performed for the isotope ratios (see panel (b) of Fig. 3). In addition, we repeated the error calculations for the complete data sets (300 s) and came to the same conclusions.

3.3.3 Signal stability

In order to study the signal stability affected by noise processes, we performed 1 h time scans of air (LUX 3588) and used the Allan variance σ^2 (Allan, 1966). This variance, which is calculated from N samples of the quantity ϕ, is given by

https://doi.org/10.5194/amt-2023-96
Preprint. Discussion started: 11 May 2023
© Author(s) 2023. CC BY 4.0 License.

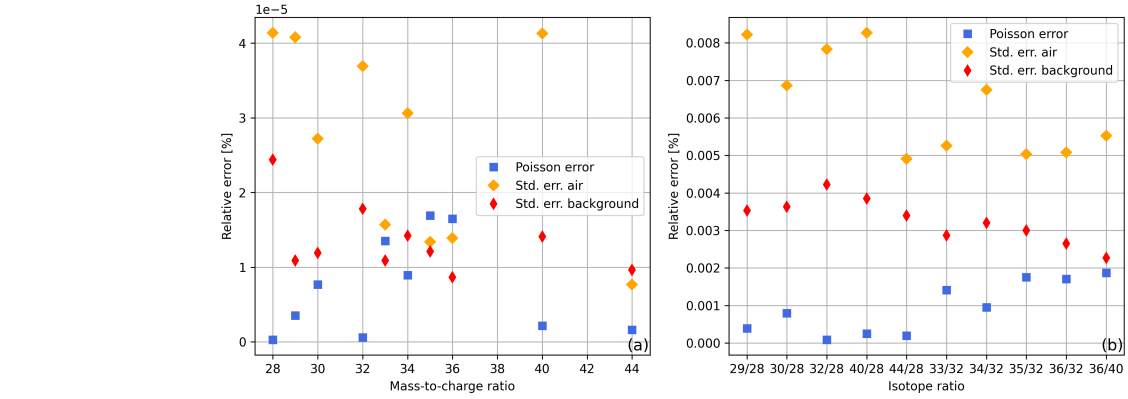

Figure 3. Relative Poisson and standard errors of (a) ion beams and (b) isotope ratios calculated from the first 60 s of the uncorrected time scans summarised in Table 1 (collector zero data for background error and air data for remaining errors). For the standard errors of the ion beams the standard deviations were divided by $\sqrt{600}$; this corresponds to the square root of the number of 0.1 s signal means we used. The relative errors of the isotope ratios $R = S_1/S_2$ were calculated by adding up the relative errors of the ion beams S_1 and S_2.

$$\sigma^2(T,\tau) = \frac{1}{N-1}\sum_{n=0}^{N-1}\left(\frac{\phi(nT+\tau)-\phi(nT)}{\tau}\right)^2 - \frac{1}{N(N-1)}\left(\sum_{n=0}^{N-1}\frac{\phi(nT+\tau)-\phi(nT)}{\tau}\right)^2. \quad (2)$$

In this equation, τ denotes the sample time and T the period of sampling. For the purpose of analysing the signal stability of different isotope ratios of air components, we considered the case $\tau = T$ (no dead time). For $\phi(t)/\tau$ we used the signal average starting at time t that we calculated for averaging times $\tau \in [1\text{ s}, 650\text{ s}]$. In Fig. 4, we present the Allan variance of the isotope ratio 34/32 as a function of the averaging time. From this figure one can see that the variance reaches its minum around (81 ± 6) s. This means that the measurement precision can be increased by signal averaging, but only up to this value. In order to get rid of the largest fluctuations, the minimum of the Allan variance was not determined from the raw data but from a centred moving average (± 10 s) of the original data set. The uncertainty of this minimum was in turn assessed by computing the standard deviation of the instants of time that were used for the calculation of the corresponding element of the moving average.

In panel (a) of Fig. 5 we report the aforementioned minima for all of the isotope ratios we usually calculate from air data. With the exception of the isotope ratios 29/28 and 40/28, this figure shows that these minima are very similar and occur at averaging times around 81 s. However, when performing five of these time scans, one finds that this minimum is quite variable. Viewed over all isotope ratios and all measurements, we found a mean value of 106 s with a standard deviation of 18 s. The individual mean values of the minima along with the corresponding standard deviations are depicted in panel (b) of Fig. 5.

https://doi.org/10.5194/amt-2023-96
Preprint. Discussion started: 11 May 2023
© Author(s) 2023. CC BY 4.0 License.

Atmospheric Measurement Techniques Discussions

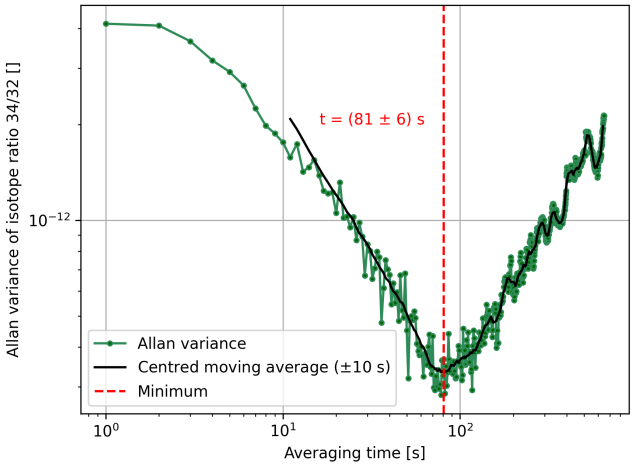

Figure 4. Allan variance of the isotope ratio 34/32 as a function of the averaging time (1 s steps). The corresponding data were recorded during a 1 h time scan of air (LUX 3588), which was performed with the Elementar isoprime precisION and the NIS-II. Furthermore, a centred moving average (±10 s) calculated from the Allan variances as well as the miniumum of the resulting curve are depicted. The uncertainty of the minimum was estimated by computing the standard deviation of the instants of time that were used for the calculation of the corresponding element of the moving average.

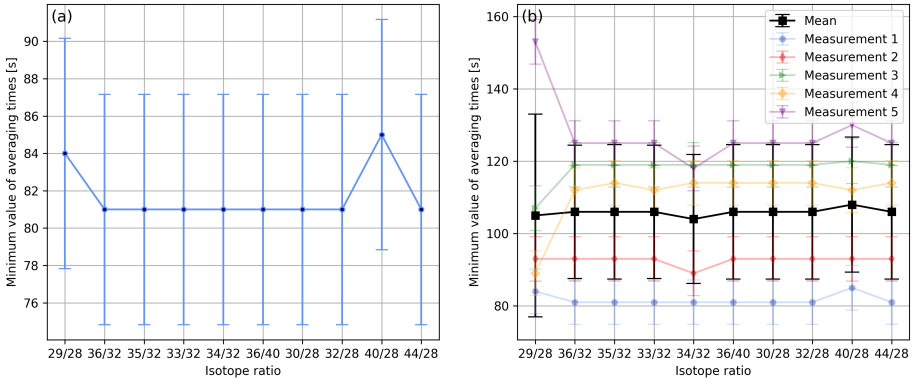

Figure 5. (a) Minimum values of averaging times of different isotope ratios determined as indicated in Fig. 4; for the calculations the same data set was used as for Fig. 4. The uncertainty of each minimum was estimated by computing the standard deviation of the instants of time that were used for the calculation of the corresponding centred moving average. (b) Minimum values of averaging times of different isotope ratios calculated from five consecutive 1 h time scans of air (LUX 3588) following the procedure depicted in (a). Furthermore, (b) shows the mean values of the minima and the corresponding standard deviations.

3.4 Comparison of different inlet systems

Besides characterising the new measurement setup we also compared the NIS-II to other inlet systems, namely to the NIS-I as well as to an Elementar iso DUAL INLET. In contrast to the former two inlet systems, the latter is a common changeover-

https://doi.org/10.5194/amt-2023-96
Preprint. Discussion started: 11 May 2023
© Author(s) 2023. CC BY 4.0 License.

Atmospheric Measurement Techniques Discussions

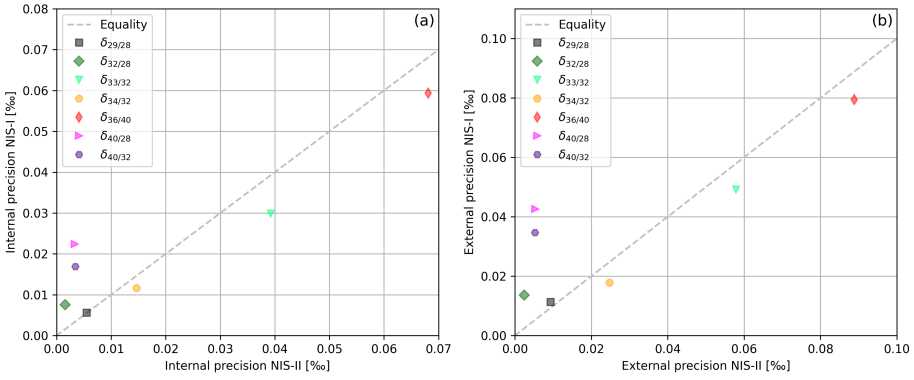

Figure 6. (a) Internal and (b) external precisions of various delta values of air components (sample cylinder LUX 3407 and standard cylinder SC 560962). For the measurements a Thermo Finnigan DELTA$^{\mathrm{plus}}$ XP with a NIS-I and a NIS-II was used; per inlet system, 50 measurements (eight delta values per measurement) were performed. The data were processed with a 2.5σ filter and $\delta_{32/28}$ as well as $\delta_{40/28}$ were corrected for drift.

valve-based dual inlet system. In the following, we will first compare measurement precisions of delta values of air components and then focus on the reproducibility of delta value means.

3.4.1 Internal and external precisions of delta values

In order to compare the NIS-II to the NIS-I we calculated correlations of internal and external precisions of various delta values of air components (see Fig. 6). The delta values were all measured with a Thermo Finnigan DELTA$^{\mathrm{plus}}$ XP IRMS on the air cylinders LUX 3407 (sample) and SC 560962 (standard). The calculation of the delta values was performed as described in appendix A, except that only consecutive standard intervals were averaged but not consecutive sample intervals. Furthermore, we applied a 2.5σ filter to the data and corrected the drift of $\delta_{32/28}$ as well as of $\delta_{40/28}$.

From Fig. 6 it can be seen that delta values of air components can be measured with very high precisions when an open-split-based dual inlet system is used; in general, these precisions are of order tenths of per meg and higher. Moreover, the data imply that for most of the delta values the NIS-II and the NIS-I provide similar results. With respect to internal precisions, the largest absolute differences are 19 $\mathrm{per\,meg}$ ($\delta_{40/28}$), 13 $\mathrm{per\,meg}$ ($\delta_{40/32}$) and 9 $\mathrm{per\,meg}$ ($\delta_{33/32}$); for the former two delta values the NIS-II was superior. Regarding the external precision, $\delta_{40/28}$ and $\delta_{40/32}$ showed the largest discrepancies again; for these delta values, the NIS-II outperformed the NIS-I by 37 $\mathrm{per\,meg}$ and 30 $\mathrm{per\,meg}$, respectively. Altogether we conclude that the modifications we made to the NIS-I had a positive influence on the measurement precision.

In addition to the comparison of our open-split-based dual inlet systems we also compared the NIS-II to the changeover-valve-based Elementar iso DUAL INLET. For this study, the Elementar isoprime precisION was used. For each inlet system, we performed 10 SA/STD measurements of compressed air. Due to the fact that with the NIS-II an additional standard gas interval was measured, the first delta value of each individual measurement was dropped; by doing this, one obtains the same

https://doi.org/10.5194/amt-2023-96
Preprint. Discussion started: 11 May 2023
© Author(s) 2023. CC BY 4.0 License.

Atmospheric Measurement Techniques Discussions

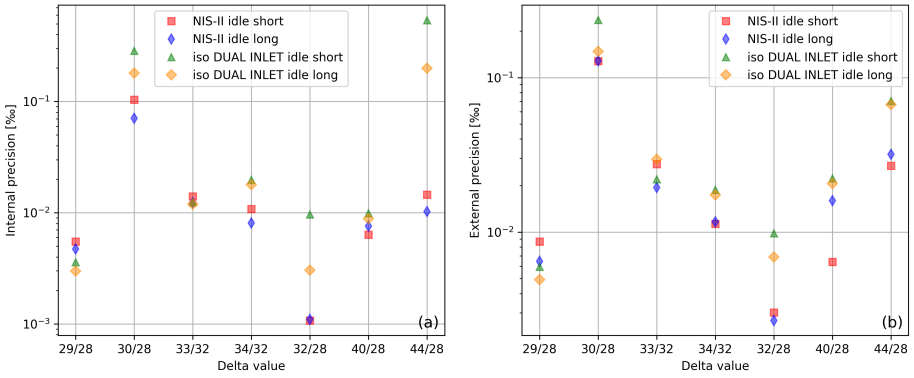

Figure 7. Internal (a) and external (b) precisions of different delta values calculated from 10 SA/STD measurements of air (standard LUX 3588 and sample LUX 3591) with the iso DUAL INLET and the NIS-II. Before each measurement with the iso DUAL INLET, the system autobalanced the $m/z = 28$ signal. The data were not corrected for non-linearity, though. The labels „idle short“ and „idle long“ refer to idle times around 20 s and 60 s, respectively.

number of delta values for both measurement series. From the collected data we determined internal and external precisions of various delta values and evaluated them for two different idle times (switch delays); the actual idle time of the measurements was around 60 s and then we reduced it to roughly 20 s by means of a processing feature of ionOS. The outcome of this study is depicted in the two panels of Fig. 7.

From Fig. 7 one learns that for most of the delta values the NIS-II provides higher internal precisions than the iso DUAL INLET. For $\delta_{29/28}$ and $\delta_{33/32}$ the latter inlet system was superior, but the differences are rather small, namely 1.7 per meg and 0.4 per meg, respectively. For the remaining delta values the NIS-II outperformed the iso DUAL INLET; the differences are in the range between 1 per meg ($\delta_{40/28}$) and 189 per meg ($\delta_{44/28}$). Regarding the external precision, only for $\delta_{29/28}$ the iso DUAL INLET was better than the NIS-II, the discrepancy is 1.5 per meg. The largest differences between the two inlet systems were observed for $\delta_{32/28}$ and $\delta_{44/28}$; these amounted to 4 per meg and 35 per meg, respectively. All of the aforementioned differences refer to an idle time of 60 s.

Furthermore, when focusing on the iso DUAL INLET, it is noticeable that with an idle time of 60 s higher precions were attained than with 20 s; the only exception is the external precision of $\delta_{33/32}$. The reason for this behaviour is that the pressure in the ion source slightly changes when the gas source is switched; as a consequence, the system needs time to re-equilibrate. For the NIS-II, however, the pressure in the ion source remains constant and thus measurements can be performed faster. When comparing the measurement results of the two idle times, for the shorter switch delay a higher internal precision was observed for 2 out of 7 delta values recorded with the NIS-II; for the external precision it is 4 out of 7. Hence, especially for the external precisions, there is no clear trend.

https://doi.org/10.5194/amt-2023-96
Preprint. Discussion started: 11 May 2023
© Author(s) 2023. CC BY 4.0 License.

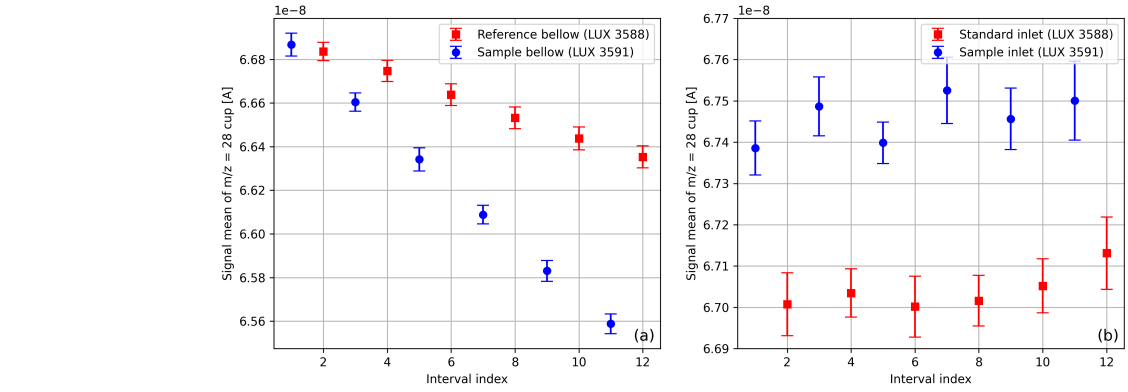

Figure 8. Average signals of $m/z = 28$ cup with standard deviations; these values were determined from 12 measuring intervals of a SA/STD measurements of compressed air (LUX 3588 and LUX 3591). The measurement depicted in (a) was carried out with the iso DUAL INLET and the one shown in (b) with the NIS-II.

3.4.2 Reproducibility of delta value means

When using the changeover-valve-based Elementar iso DUAL INLET it can be observed that the beam intensity declines as a function of time. When a single SA/STD measurement of compressed air is carried out this decrease usually presents itself as depicted in panel (a) of Fig. 8. The origin of this decline is the steady consumption of gas, which results in a gradual reduction of the gas pressure inside of the bellows. Moreover, panel (a) of Fig. 8 makes it clear that the $m/z = 28$ signals of the gas stored in the two bellows decrease differently. One reason for this is that the reference bellow is larger than sample below and the other that the corresponding feeding capillaries are not crimped identically. In order to prevent this decrease from propagating further, before each individual measurement of a measurement series, the bellows are autobalanced with respect to a predefined signal height; for air and oxygen measurements this autobalancing is performed with respect to the $m/z = 28$ and $m/z = 32$ signals, respectively.

In contrast, panel (b) of Fig. 8 points out that data gathered with the NIS-II do not show a signal decrease. The NIS-II was designed in such a way that sample and standard gas cylinders can be directly connected to the inlet system; because the gas pressure of the NIS-II is regulated the signals remain approximately constant.

Due to the previously mentioned observations, we typically correct the iso DUAL INLET data for non-linearity. This correction is necessary because the IRMS was tuned with respect to maximum sensitivity instead of linearity. For SA/STD measurements we determine this correction as follows:

1. We select the isotope ratio we would like to correct and separate the mean values of the standard from the sample intervals; the same is done for the interval means of the $m/z = 28$ area (integral of $m/z = 28$ signals), which is used as an indicator of the signal decrease.

https://doi.org/10.5194/amt-2023-96
Preprint. Discussion started: 11 May 2023
© Author(s) 2023. CC BY 4.0 License.

Atmospheric Measurement Techniques Discussions

2. Next, the $m/z = 28$ area of the first standard interval (reference interval) is subtracted from the consecutive standard interval means. Afterwards, the isotope ratio means of the standard gas are plotted against these area differences; in order to estimate their change we use a linear regression (see Fig. 9). In general, we try to obtain coefficients of determination of at least 0.7; if this coefficient is distinctly lower than this value, we try to improve the fit by shifting the point of reference from the first interval to a later interval (all intervals before the point of reference are dropped). We then repeat this procedure for the sample intervals.

3. In order to correct the isotope ratio means of the standard intervals, the slope of the linear regression of the standard intervals (see step 2) is multiplied by the $m/z = 28$ area differences of the individual standard intervals; these products describe the absolute changes of the isotope ratio and have to be subtracted from the isotope ratio means of the respective intervals. As before, the same procedure has to be repeated for the sample intervals.

4. Before calculating delta values from the corrected isotope ratios, a further correction has to be applied. This is necessary because the area differences are calculated for sample and standard intervals separately; as a result, the two reference intervals do not refer to the same point in time (different signal heights). If the standard reference interval was measured after the reference interval of the sample, we linearly interpolate the $m/z = 28$ area differences of the standard intervals; this interpolation allows to determine the area difference at the time the sample reference interval was measured. After multiplying this difference by the slope of the linear regression of standard intervals computed in step 2, this product has to be added to all of the isotope ratio means of the standard intervals. In case that the sample reference interval was measured after the standard reference interval, this correction procedure has to be applied to the sample intervals.

If we calculate delta values directly from the ion beam data (0.1 s resolution) instead of relying on the interval means provided by ionOS, we first separate sample from standard data points, remove the data points recorded during idle periods (normally the first 20 s of each interval), calculate linear regressions for the remaining ion beam data (for sample and standard intervals separately) and then correct this data accordingly; in order to compute isotope ratios, delta values and their uncertainties, we use the corrected ion beam data to calculate the signal areas of the different intervals and then follow the principles stated in Appendix A.

In Fig. 10 we present interval means of $\delta_{32/28}$ and $\delta_{40/28}$, which we recorded during two air measurements with the isoprime precisION; one was performed with the NIS-II and the other with the iso DUAL INLET. As can be seen from this figure, despite the application of a non-linearity correction the two inlet systems lead to appreciably different results. Therefore, we determined these delta values with another NIS-II that was connected to a Thermo Finnigan DELTA$^{\mathrm{plus}}$ XP (see Table 2). For measurements with this setup we chose an integration time of 10 s and an idle time of 20 s. In contrast to the measurements with the isoprime precisION, the air cylinders LUX 3588 and LUX 3591 were not measured against each other, but against an in-house standard. However, as the same in-house standard was used for both cylinders, the delta values referring to LUX 3591 (sample) against LUX 3588 (standard) could be calculated from this data. In order to improve the measurement results we

https://doi.org/10.5194/amt-2023-96
Preprint. Discussion started: 11 May 2023
© Author(s) 2023. CC BY 4.0 License.

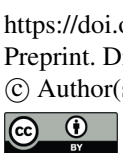

Atmospheric Measurement Techniques Discussions

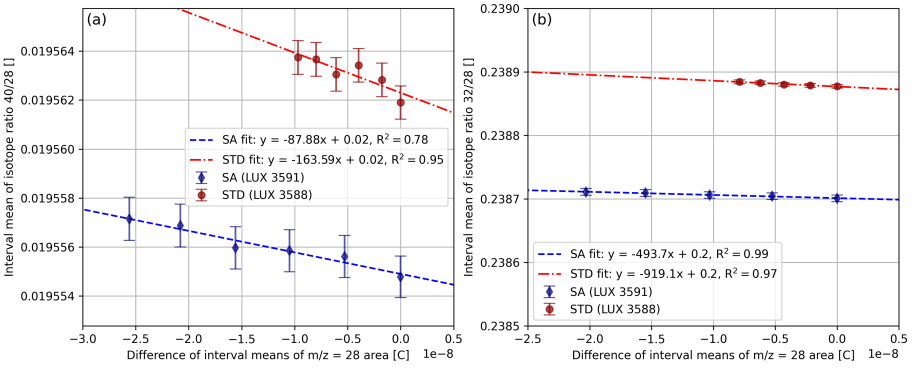

Figure 9. Interval means of the isotope ratios (a) 40/28 and (b) 32/28 as a function of $m/z = 28$ area differences (see step 2 of description of non-linearity correction). The ratios were recorded during a SA/STD measurement of compressed air (LUX 3588 and LUX 3591) with the iso DUAL INLET. The error bars indicate measurement uncertainties estimated by means of Eq. (A5).

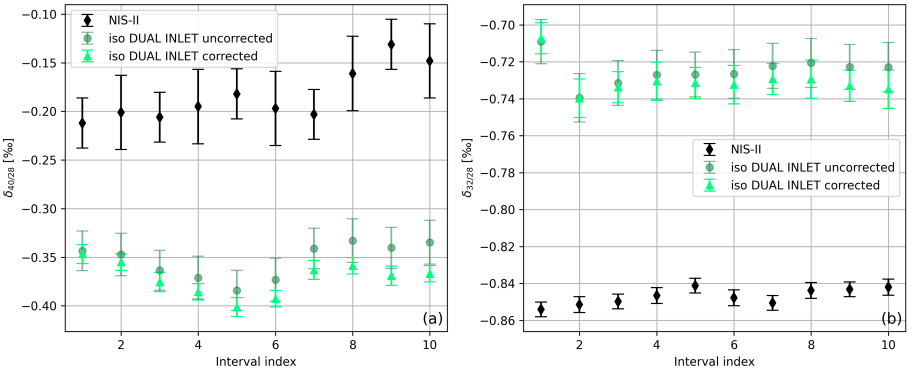

Figure 10. (a) Mean values of $\delta_{40/28}$ and (b) $\delta_{32/28}$ recorded during two SA/STD measurements of compressed air (standard cylinder LUX 3588 and sample cylinder LUX 3591); one of the measurements was performed with the NIS-II and the other with the iso DUAL INLET. For both measurements an idle time around 60 s was used. The uncertainties of the delta values were estimated by means of the propagation of uncertainty (see appendix A). The non-linearity correction applied to data labelled as „corrected“ follows the principle described in the main text of this section.

375 applied a 2.5σ filter and a drift correction to the data.

Table 2 points out that measurements carried out with different mass spectrometers can be reproduced quite precisely if the NIS-II is used. Regarding $\delta_{40/28}$, the mean values measured with the isoprime precisION and the DELTA$^{\mathrm{plus}}$ XP differ by approximately 2 $\mathrm{per\,meg}$. For $\delta_{32/28}$ the deviation is around 25 $\mathrm{per\,meg}$. Although both discrepancies are rather small, for
380 $\delta_{32/28}$ it is not within the measurement uncertainty; this difference might be caused by minor adsorption/desorption effects on inside surfaces of the two mass sprectrometers. For the NIS-I the reproducibilities of $\delta_{32/28}$ and $\delta_{40/28}$ were reported to

https://doi.org/10.5194/amt-2023-96
Preprint. Discussion started: 11 May 2023
© Author(s) 2023. CC BY 4.0 License.

Atmospheric Measurement Techniques Discussions

Table 2. Mean values of $\delta_{32/28}$ and $\delta_{40/28}$ along with external precisions measured on compressed air (standard cylinder LUX 3588 and sample cylinder LUX 3591). These delta values were obtained with an Elementar isoprime precisION and a Thermo Finnigan DELTA^{plus} XP (measurement and data processing procedures as described in main text); as inlet systems a NIS-II and a Elementar iso DUAL INLET (autobalancing enabled) were used. The non-linearity correction applied to data labelled as „corrected“ was calculated on the basis of the interval means provided by ionOS. For measurements with the DELTA^{plus} XP, 94 delta values from 13 SA/STD measurements were evaluated; regarding the isoprime precisION, for each inlet system, 100 delta values from 10 consecutive SA/STD measurements were taken into consideration.

Mass spectrometer	Dual inlet system	$\delta_{32/28}$[‰]	$\delta_{40/28}$[‰]
Thermo Finnigan Delta Plus XP	NIS-II	-0.871 ± 0.003	-0.204 ± 0.008
Elementar isoprime precisION	NIS-II	-0.846 ± 0.003	-0.206 ± 0.016
Elementar isoprime precisION	iso DUAL INLET uncorrected	-0.737 ± 0.007	-0.380 ± 0.021
Elementar isoprime precisION	iso DUAL INLET corrected	-0.748 ± 0.013	-0.401 ± 0.041

be lower than 5 $\mathrm{per\,meg}$ and 20 $\mathrm{per\,meg}$, respectively (Leuenberger, 2000). The authors state that for this comparision the corresponding data were compared to an air standard, which was calibrated by means of free atmospheric air.

Delta values obtained with the isoprime precisION and the iso DUAL INLET, show larger deviations from the mean values recorded with the DELTA^{plus} XP; for $\delta_{32/28}$ the discrepancy of the mean values is roughly 134 $\mathrm{per\,meg}$ and for $\delta_{40/28}$ about 176 $\mathrm{per\,meg}$. Moreover, the external precisions of the iso DUAL INLET data are significanly lower. As can be seen in the last row of Table 2, the application of a non-linearity correction to this data reduces the deviation of the $\delta_{32/28}$ means, whereas for $\delta_{40/28}$ the discrepancy slightly increases. On the one hand, this correction also improves the internal precisions, namely by factor of 3 for $\delta_{32/28}$ and by a factor of 2 for $\delta_{40/28}$, on the other hand, the external precisions deteriorate by a factor of 2 (see Table 2). The non-linearity correction normally influences internal precisions the strongest because the autobalancing of the bellows is only performed at the start of each measurement and not inbetween measuring intervals.

Last but not least, it is worth focusing on the measurement duration. In general, more measurements have to be performed with the iso DUAL INLET than with the NIS-II to obtain comparable external precisions (see Fig. 7; this in turn translates into an additional expenditure of time. For instance, for measurements of $\delta_{32/28}$ with the iso DUAL INLET, a measurement series consisting of 10 SA/STD measurements would have to be repeated more than 5 times (calculation based on Table 2).

3.5 Feasibility study of clumped isotope measurements of air components

As stated in the introduction, one of our main goals was to determine whether our measurement setup allowed to measure clumped isotopes of air components or not. In general, for such measurements the following requirements have to be met (Eiler, 2007):

https://doi.org/10.5194/amt-2023-96
Preprint. Discussion started: 11 May 2023
© Author(s) 2023. CC BY 4.0 License.

Atmospheric Measurement Techniques Discussions

- High mass resolution: mass spectrometers with a low mass resolution may not be able to resolve isobaric interferences. In some cases, high mass resolving power can be compensated by high sample purity.
- High abundance sensitivity: the abundance of clumped isotopes is typically much smaller than the abundance of singly-substituted isotopologues and thus a high abundance sensitivity is required.
- High measurement precision: typically, the required measurement precision is of order 10^{-5} and higher.
- Preservation of the original molecular bonds: alteration of molecular bonds during the measurement procedure or sample handling may modify the clumped isotope signals.

In the following discussion we only touch upon the first three of these basic requirements because they are directly related to the mass spectrometer and its inlet system. In contrast, the integrity of the original bonds also depends on other factors.

3.5.1 Mass resolution

Due to the fact that the mass resolution of the Elementar isoprime precisION is merely around 110 $\mathrm{m}\,\Delta\mathrm{m}^{-1}$ (Elementar, 2022) resolving isobaric interferences is not possible. For instance, Laskar (2019) use a Thermo Scientific 253 Ultra High Resolution (HR) IRMS with a medium mass resolution of 10000 $\mathrm{m}\,\Delta\mathrm{m}^{-1}$ in order to discriminate between $^{36}\mathrm{Ar}$, $\mathrm{H}^{35}\mathrm{Cl}$ and $^{18}\mathrm{O}^{18}\mathrm{O}$. Despite the fact that air measurements with the isoprime precision produce a well-defined $m/z = 36$ peak, it is not possible to tell these three components apart, though. Neither is it possible to distinguish the clumped isotope $^{17}\mathrm{O}^{17}\mathrm{O}$ from the singly-substituted isotopologue $^{16}\mathrm{O}^{18}\mathrm{O}$ or $^{17}\mathrm{O}^{18}\mathrm{O}$ from $^{35}\mathrm{Cl}$.

Due to the limited mass resolution of our IRMS we concluded that the feasibility study regarding clumped isotope measurements of air components cannot be focused on air but must be performed on the pure gases air is composed of. In what follows, we present measurements of pure oxygen gas; we decided to focus on oxygen because it has multiple clumped isotopes and because our Faraday collector array has all of the required cups. In addition, clumped isotope measurements of oxygen have already been published by other groups such that comparisons can be drawn.

As an aside, it may be mentioned that also molecular nitrogen was a potential candidate for our study because the abundance of $^{15}\mathrm{N}^{15}\mathrm{N}$ in N_2 is more than 3 times higher than the abundance of $^{18}\mathrm{O}^{18}\mathrm{O}$ in O_2 (Meija, 2016). However, $^{15}\mathrm{N}^{15}\mathrm{N}$ is the only clumped isotope of nitrogen, which makes it less suitable for our purpose.

3.5.2 Abundance sensitivity

The AV scan depicted in panel (a) of Fig. 11 proves that our setup is sensitive enough to detect $^{17}\mathrm{O}^{18}\mathrm{O}$ ($m/z = 35$) and $^{18}\mathrm{O}^{18}\mathrm{O}$ ($m/z = 36$) in pure oxygen gas. Nevertheless, if the collector zeros are subtracted from these signals (around $1 \cdot 10^{-11}$ A) they both become negative; this eventually leads to incorrect delta values. Hence, the collector zeros do not represent the correct background of these signals.

https://doi.org/10.5194/amt-2023-96
Preprint. Discussion started: 11 May 2023
© Author(s) 2023. CC BY 4.0 License.

Atmospheric Measurement Techniques Discussions

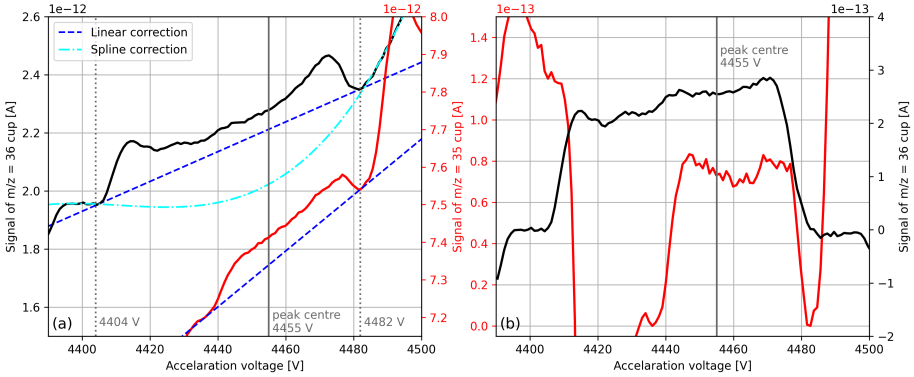

Figure 11. (a) Raw signals of the mass-to-charge ratios 35 and 36 around the measurement position (peak centre). The signals were both recorded during a single AV scan of pure oxygen gas (cylinder SC 62349), which was performed with the isoprime precisION and the NIS-II. Besides the peak centre, suitable positions for background corrections (dotted lines) and the corresponding correction functions are indicated. (b) Corrected signals of the mass-to-charge ratios 35 and 36. For the former signal, the linear correction depicted in panel (a) was used and for the latter the spline correction.

On Faraday cups measuring clumped isotopes usually a negative background is visible, which is created by secondary electrons (Bernasconi, 2013). Furthermore, it is known that this background can lead to non-linearity effects and that the amount of secondary electrons is positively correlated with the amount of gas that is admitted to the mass spectrometer (Bernasconi, 2013). In order to reduce this background we connected an external power supply to our IRMS and applied a suppressor voltage of -140 V to its Faraday cups. By default, this voltage is set to approximately -38 V (Elementar, 2017). Measurements with the isoprime precisION have shown that the application of a much lower voltage does not make sense because the signals start to saturate around -100 V (see Fig. 12). Unfortunately, the application of a suppressor voltage alone is not enough to generate positive $m/z = 35$ and $m/z = 36$ signals. As suggested by Bernasconi (2013), in order to solve this issue a background value in the presence of the analyte has to be determined.

One option presented by Bernasconi (2013) is to infer the background from the main mass component of the analyte gas ($m/z = 32$ for oxygen). In order to determine the relationships between different Faraday cup signals at different acceleration voltages and at varying pressure levels we carried out a series of AV scans. For this measurement series we filled the reference bellow of the iso DUAL INLET with pure oxygen (SC 540546), maximised the signal by means of bellow compression and then performed an AV scan every 30 min without readjusting the bellow. In order to measure over a considerable range of source pressures, these scans were performed over a period of 3 days; in this period of time the $m/z = 32$ signal declined from approximately $9.4 \cdot 10^{-8}$ A to $5.4 \cdot 10^{-9}$ A.

In order to estimate the background of the $m/z = 35$ peak we first inspected the AV scans to determine positions that represent the background appropriately; due to the fact that the peak was not flat but growing as a function of the acceleration voltage we selected two positions, namely one before the peak and one after it (see panel (a) of Fig. 11). By means of correlation plots created on the basis of the AV scans we then inferred the signal at these two positions from linear fits; as predictor we

https://doi.org/10.5194/amt-2023-96
Preprint. Discussion started: 11 May 2023
© Author(s) 2023. CC BY 4.0 License.

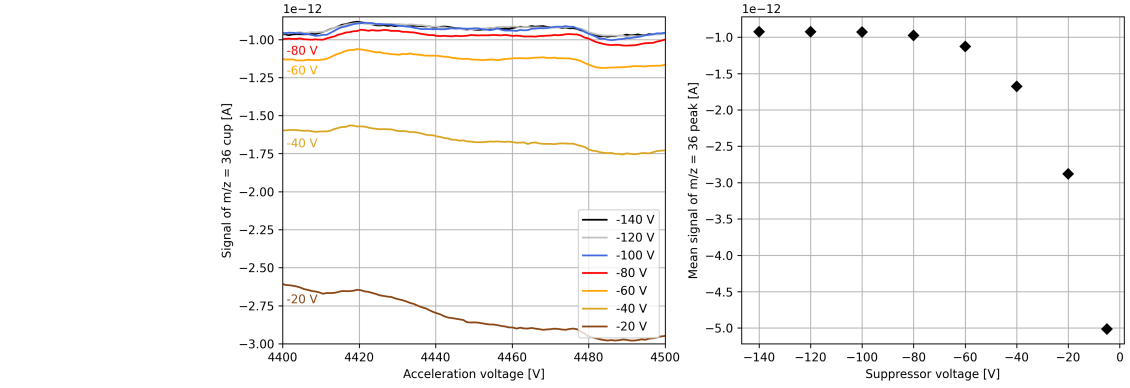

Figure 12. (a) Signals of the $m/z = 36$ cup recorded during acceleration voltage scans of pure oxygen gas (cylinder SC 84567). These scans were carried out at different suppressor voltages and the gas was admitted to the isoprime precisION by means of the NIS-II. (b) Mean signals of the $m/z = 36$ peak as a function of the suppressor voltage. The means were calculated from extracts of the curves in (a), namely in the range between 4440 V and 4480 V.

first tested the peak centre (measurement position) of the $m/z = 32$ signal, which provided coefficients of determination around 0.996. After linearly interpolating the two background values and subtracting the value at the peak centre from the $m/z = 35$ signal we eventually obtained a positive value. During regular SA/STD measurements this correction is applied to the individual interval means after the collector zero correction has been removed.

Later, we tested other correlations as well and noticed that using the peak centre of the $m/z = 35$ signal as predictor for the $m/z = 35$ background does not only provide better fits ($R^2 \approx 0.99993$) but also better results in terms of the accuracy of the isotope ratio 35/32. Please note that the $m/z = 32$ signal was still corrected by subtracting the collector zero value; the justification for this is that the $m/z = 32$ signal ($6.8 \cdot 10^{-8}$ A) is distinctly higher than the collector zero value ($1.0 \cdot 10^{-9}$ A).

We repeated the same correction procedure for $m/z = 36$ and also here the peak centre of the $m/z = 36$ signal predicted its background the best. However, as can be seen from panel (a) of Fig. 11, for $m/z = 36$ the linear correction is not ideal because the peak top is not flat. In order to take the curvature of the peak top into account we calculated an appropriate spline. Instead of repeating this calculation for every SA/STD measurement we compute the linear correction for each of its interval means and then improve the correction by adding a constant value; this value, which corresponds to the difference between the spline and the linear correction, is deduced from a single AV scan (see panel (b) of Fig. 11). In order to monitor the background of the peaks, before each measurement series an AV scan is performed; when major changes are observed, the corrections are recalculated.

https://doi.org/10.5194/amt-2023-96
Preprint. Discussion started: 11 May 2023
© Author(s) 2023. CC BY 4.0 License.

Atmospheric Measurement Techniques Discussions

Table 3. Ranges of oxygen isotope abundances observed in natural materials (Meija, 2016) along with abundances of oxygen isotopologues calculated from the observed oxygen isotope abundances (last six rows).

Cardinal mass [u]	Isotopes/Isotopologues	Range of relative abundances
16	^{16}O	[99.738 %, 99.776 %]
17	^{17}O	[0.367 ‰, 0.400 ‰]
18	^{18}O	[0.187 %, 0.222 %]
32	$^{16}O^{16}O$	[99.477 %, 99.553 %]
33	$^{16}O^{17}O$, $^{17}O^{16}O$	[366.0 ppm, 399.1 ppm]
34	$^{16}O^{18}O$, $^{18}O^{16}O$	[0.187 %, 0.222 %]
34	$^{17}O^{17}O$	[0.1 ppm, 0.2 ppm]
35	$^{17}O^{18}O$, $^{18}O^{17}O$	[0.7 ppm, 0.9 ppm]
36	$^{18}O^{18}O$	[3.5 ppm, 4.9 ppm]

3.5.3 Measurement precision

Since oxygen has two heavy isotopes, namely ^{17}O and ^{18}O, any combination of these isotopes is a clumped isotope of molecular oxygen. In Table 3 ranges of oxygen isotope abundances observed in natural materials are shown as well as the corresponding abundances of oxygen isotopologues.

Due to the fact that oxygen isotope ratios are calculated with respect to $^{16}O^{16}O$, whose relative abundance is almost equal to one, the minimum measurement precision that is required to measure a certain isotope ratio is very similar to the relative abundance of the rare isotope. This implies that for the isotope ratios 35/32 and 36/32 external precisions of at least $7 \cdot 10^{-7}$ and $3.5 \cdot 10^{-6}$, respectively, have to be achieved (see Table 3).

In Table 4 external precisions of oxygen isotope ratios and their delta values are shown; these were calculated from 10 SA/STD measurements of pure oxygen, which we performed with the isoprime precisION and the NIS-II. The $m/z = 32$ signals were corrected by means of the collector zero value and the clumped isotope signals according to the correlation method described in Sect. 3.5.2. When calculating the standard deviation of the 60 sample interval means one obtains $3.4 \cdot 10^{-9}$ for 35/32 and $4.9 \cdot 10^{-9}$ for 36/32; these precisions are more than 2 orders of magnitude higher than the minimum requirements.

Furthermore, in Table 4 we compare our measurements to those reported by Laskar (2019) (supplementary material), which performed clumped isotope measurements on atmospheric oxygen with a Thermo Scientific 253 Ultra High Resolution IRMS. With the exception of the isotope ratio 35/32 higher precisions were obtained with the Elementar isoprime precisION. For the isotope ratio 35/32 the difference between the two mass spectrometers is relatively small, though, namely roughly $5 \cdot 10^{-10}$.

Please note that for both data sets depicted in Table 4 the same amount of data points (60 independent interval means) was taken into consideration. Additionally, the standard deviations of the isoprime precisION were divided by $\sqrt{67/20}$ since Laskar (2019) integrated over 67 s instead of 20 s.

https://doi.org/10.5194/amt-2023-96
Preprint. Discussion started: 11 May 2023
© Author(s) 2023. CC BY 4.0 License.

Atmospheric Measurement Techniques Discussions

Table 4. Standard deviations of oxygen isotope ratios and delta values calculated from 60 independent interval means of pure oxygen gas measurements. In the second column, data collected with the Elementar isoprime precisION and the NIS-II are shown; the precisions were calculated from 10 SA/STD measurements (sample cylinder SC 540546 and standard cylinder SC 62349) and the data were corrected as described in Sect. 3.5.2. In the third column, data published by Laskar (2019) (supplementary material) is presented. They measured purified oxygen (extracted from atmospheric air) against the working gas IMAU O_2 with a Thermo Scientific 253 Ultra High Resolution IRMS. The reported precisions were calculated from 10 of these measurements, whereby pressure corrections were applied to $\delta_{33/32}$ and $\delta_{34/32}$. Since Laskar (2019) integrated over 67 s and not over 20 s the standard deviations of the isoprime precisION data were divided by $\sqrt{67/20}$.

Parameter	Elementar isoprime precisION	Thermo Scientific 253 Ultra HR
33/32	$5.6 \cdot 10^{-8}$	$1.0 \cdot 10^{-7}$
34/32	$4.7 \cdot 10^{-7}$	$1.2 \cdot 10^{-6}$
35/32	$1.8 \cdot 10^{-9}$	$1.3 \cdot 10^{-9}$
36/32	$2.7 \cdot 10^{-9}$	$3.5 \cdot 10^{-9}$
$\delta_{33/32}$	0.011 ‰	0.064 ‰
$\delta_{34/32}$	0.016 ‰	0.061 ‰
$\delta_{35/32}$	0.145 ‰	0.926 ‰
$\delta_{36/32}$	0.214 ‰	0.684 ‰

4 Conclusions

The operation of the NIS-II for more than a year has shown that this dual inlet system requires significantly less maintenance than the NIS-I; thanks to the new capillary switching mechanism and the straight open split only very few hours have to be spent for maintenance per year. Furthermore, using a straight glass tube instead of a Y-shaped piece as open split interface is beneficial because installation is much faster and gas-tightness is superior. With regard to measurement performance, the largest differences between the NIS-I and the NIS-II were observed for the external precisions of $\delta_{40/28}$ and $\delta_{40/32}$; for these delta values, the precision of the NIS-II was higher by 37 $\mathrm{per\,meg}$ and 30 $\mathrm{per\,meg}$ (50 measurements), respectively.

Moreover, we compared the NIS-II to an Elementar iso DUAL INLET and demonstrated that data recorded with the former inlet system do not require non-linearity corrections if the amount of gas is not limited. On the other hand, the sample consumption of the NIS-II is higher than that of the Elementar iso DUAL INLET. By means of SA/STD measurements of air we also showed that, in general, higher measurement precisions can be attained with the NIS-II. Only for $\delta_{29/28}$ the iso DUAL INLET yielded significantly higher precisions; for 10 SA/STD measurements with an idle time of 60 s and autobalancing of the iso DUAL INLET's bellows the external and internal precisions of the two inlet systems differed by up to 1.5 $\mathrm{per\,meg}$ and 1.7 $\mathrm{per\,meg}$, respectively. For the remaining delta values the NIS-II outperformed the iso DUAL INLET; for the internal pre-

https://doi.org/10.5194/amt-2023-96
Preprint. Discussion started: 11 May 2023
© Author(s) 2023. CC BY 4.0 License.

Atmospheric Measurement Techniques Discussions

cisions the observed differences are in the range between 1 per meg and 189 per meg and for the external precisions between 3 per meg and 35 per meg. All of the previously mentioned differences refer to data that were not corrected for non-linearity.

In addition, we compared these air measurements to measurements performed with a Thermo Finnigan DELTA$^{\mathrm{plus}}$ XP. In this comparison we focused on the delta values $\delta_{32/28}$ and $\delta_{40/28}$ and found that their mean values can be reproduced more precisely with the NIS-II. This was especially noticeable for measurements of $\delta_{40/28}$ where the difference of the mean values was merely around 2 per meg; in contrast, the mean values determined with the isoprime precisION and the iso DUAL INLET deviated around 0.2 ‰ from the mean value of the Thermo Finnigan device.

By means of measurements of the isotope ratios 35/32 and 36/32 on pure oxygen gas we also demonstrated that with the Elementar isoprime precision and the NIS-II clumped isotope studies on pure gases are feasible; for these two ratios we attained precisions that are over 2 orders of magnitude higher than the required minimum values. In addition we showed that in terms of precision our setup is able to keep up with the Thermo Scientific 253 Ultra High Resolution IRMS. Due to the low mass resolution of the Elementar isoprime precisION and the existence of isobaric interferences, though, clumped isotope measurements can only be performed on pure gases or gas mixtures without isobaric interferences.

Due to the auspicious results we are now attempting to perform clumped isotope measurements according to common practices including the heating of gas samples. Furthermore, we are currently improving our background correction routine because the mean values of the isotope ratios 35/32 and 36/32 are still lacking a proper calibration.

Code and data availability. The data and code are both available upon request (stephan.raess@unibe.ch).

Appendix A: Calculation of isotope ratios and delta values

The software of the Elementar isoprime precisION, ionOS, calculates delta values by making use of three consecutive isotope ratio means; on condition that a SA/STD measurement is composed of 12 measuring intervals (six standard and six sample measurements performed in alternating order) and that the resulting isotope ratios means are denoted by R_i ($i \in [1,12]$), the first delta value is calculated as follows:

$$\delta_1(‰) = \left(\frac{R_2}{\frac{R_1+R_3}{2}} - 1 \right) \cdot 1000\,‰. \tag{A1}$$

In analogy to the first delta value, the second one is given by

$$\delta_2(‰) = \left(\frac{\frac{R_2+R_4}{2}}{R_3} - 1 \right) \cdot 1000\,‰. \tag{A2}$$

https://doi.org/10.5194/amt-2023-96
Preprint. Discussion started: 11 May 2023
© Author(s) 2023. CC BY 4.0 License.

Atmospheric Measurement Techniques Discussions

The delta values of the subsequent measuring intervals are computed accordingly.

When applying the propagation of uncertainty to Eq. (A1), one obtains the following expression for the uncertainty of δ_1:

$$\begin{aligned}\Delta\delta_1(‰) = \Bigg[& \left(\frac{-2000 \cdot R_2}{(R_1+R_3)^2} \cdot \Delta R_1\right)^2 + \left(\frac{2000}{R_1+R_3} \cdot \Delta R_2\right)^2 \\ & + \left(\frac{-2000 \cdot R_2}{(R_1+R_3)^2} \cdot \Delta R_3\right)^2 \\ & - \frac{4 \cdot 10^6 \cdot R_2}{(R_1+R_3)^3} \cdot \Delta R_1 \cdot \Delta R_2 \cdot \rho_{R_1,R_2} \\ & + \frac{4 \cdot 10^6 \cdot R_2^2}{(R_1+R_3)^4} \cdot \Delta R_1 \cdot \Delta R_3 \cdot \rho_{R_1,R_3} \\ & - \frac{4 \cdot 10^6 \cdot R_2}{(R_1+R_3)^3} \cdot \Delta R_2 \cdot \Delta R_3 \cdot \rho_{R_2,R_3} \Bigg]^{\frac{1}{2}} ‰. \end{aligned} \tag{A3}$$

A repetition of this calculation for Eq. (A2) yields

$$\begin{aligned}\Delta\delta_2(‰) = \Bigg[& \left(\frac{500}{R_3} \cdot \Delta R_2\right)^2 + \left(\frac{-500 \cdot (R_2+R_4)}{R_3^2} \cdot \Delta R_3\right)^2 \\ & + \left(\frac{500}{R_3} \cdot \Delta R_4\right)^2 \\ & - \frac{2.5 \cdot 10^5 \cdot (R_2+R_4)}{R_3^3} \cdot \Delta R_2 \cdot \Delta R_3 \cdot \rho_R \\ & + \frac{2.5 \cdot 10^5}{R_3^2} \cdot \Delta R_2 \cdot \Delta R_4 \cdot \rho_R \\ & - \frac{2.5 \cdot 10^5 \cdot (R_2+R_4)}{R_3^3} \cdot \Delta R_3 \cdot \Delta R_4 \cdot \rho_R \Bigg]^{\frac{1}{2}} ‰. \end{aligned} \tag{A4}$$

In Eq. (A3) and Eq. (A4), ΔR_i denotes the uncertainty of the isotope ratio mean of the measuring interval i and ρ_R the correlation coefficient (identical for all $\Delta\delta_i$); for ρ_R we use the correlation between the six standard and the six sample ratios (averaging of sample and standard isotope ratio means taken into account).

Due to the fact that ionOS does not provide the uncertainties of the isotope ratios ΔR_i, we compute them with the help of the propagation of uncertainty as well. When denoting the signal area in the isotope ratios' numerator by A_i (uncertainty ΔA_i), the one in its denominator by B_i (uncertainty ΔB_i) and the correlation coefficient of these areas by ρ_{A_i,B_i}, the uncertainty of the isotope ratio $R_i = A_i/B_i$ is given by

https://doi.org/10.5194/amt-2023-96
Preprint. Discussion started: 11 May 2023
© Author(s) 2023. CC BY 4.0 License.

Atmospheric Measurement Techniques Discussions

$$\Delta R_i = R_i \cdot \left[\left(\frac{\Delta A_i}{A_i} \right)^2 + \left(\frac{\Delta B_i}{B_i} \right)^2 - 2 \cdot \rho_{A_i,B_i} \cdot \left(\frac{\Delta A_i \cdot \Delta B_i}{A_i \cdot B_i} \right) \right]^{\frac{1}{2}}. \tag{A5}$$

For ΔA_i and ΔB_i we generally use standard deviations; for standard intervals (odd i) we calculate the standard deviation of the six standard interval areas and then repeat the calculation for the sample intervals (even i). Similarly, we only calculate one correlation coefficient per gas, namely by computing the correlation between the six A_i and the six B_i of the corresponding gas. Hence, not every ΔR_i gets different ΔA_i, ΔB_i and ρ_{A_i,B_i} but standard and sample intervals do.

Author contributions. SR was in charge of investigation. PN and WP provided technical support. The formal analysis and validation of the thereby generated data were carried out by SR and ML. MS performed the measurements with the Thermo Finnigan DELTA$^{\text{plus}}$ XP as well as the formal analysis of the data he collected. In the instrument development ML, PN and various members of the workshop teams of the Climate and Environmental Physics Division of the University of Bern were involved. SR was in charge of visualisation and wrote the original draft of the paper. In the reviewing and editing process SR, ML, PN and PW were involved. For funding acquisition ML and PW were responsible.

Competing interests. The authors declare that they have no conflict of interest.

Acknowledgements. First of all, we would like to express our gratitude to Elementar Analysensysteme GmbH, Elementar-Straße 1, D-63505 Langenselbold, Germany and in particular the Elementar UK Ltd., Isoprime House, Earl Road, Cheadle Hulme, Stockport - SK8 6PT, United Kingdom who provided financial support for this work. We would also like to thank the Swiss National Science Foundation (SNF-Project 172550) that contributed financial resources as well. Furthermore, we would like to sincerely thank the members of the workshop teams of the Climate and Environmental Physics Division of the University of Bern whose effort regarding the design, development and maintenance of the open-split-based dual inlet system was indispensable. Last but not least a special thank you goes to Dr. Michael Schibig who performed and evaluated the measurements with the Thermo Finnigan DELTA$^{\text{plus}}$ XP.

https://doi.org/10.5194/amt-2023-96
Preprint. Discussion started: 11 May 2023
© Author(s) 2023. CC BY 4.0 License.

References

Allan, D. W.: Statistics of atomic frequency standards, P. IEEE, 54, 221-230, https://doi.org/10.1109/PROC.1966.4634, 1966

Bernasconi, S. M., Hu, B., Wacker, U., Fiebig, J., Breitenbach, S. F., and Rutz, T.: Background effects on Faraday collectors in gas-source mass spectrometry and implications for clumped isotope measurements, Rapid Communications in Mass Spectrometry, 27, 603-612, https://doi.org/10.1002/rcm.6490, 2013

Brand, W. A.: PreCon: a fully automated interface for the Pre-Gc concentration of trace gases on air for isotopic analysis, Isot. Environ. Healt. S., 31, 277-284, 1995

Eiler, J. M.: „Clumped-isotope" geochemistry – The study of naturally-occurring, multiply-substituted isotopologues, Earth and planetary science letters, 262, 309-327, https://doi.org/10.1016/j.epsl.2007.08.020, 2007

Elementar Analysensysteme GmbH: isoprime precisION User Manual A comprehensive user manual describing how to work with an isoprime precisION system, http://support.elementar.co.uk/documentation/Subsystems/ precisION/manuals/, 2017

Elementar Analysensysteme GmbH: isoprime precisION The most flexible IRMS ever created, Art.-No. 05 005 646, 03 / 2022 A, https://www.elementar.com/de/produkte/stabilisotopenanalysatoren/ massenspektrometer/isoprime-precision, 2022

Keeling, R. F. and Graven, H. D.: Insights from Time Series of Atmospheric Carbon Dioxide and Related Tracers, Annu. Rev. Env. Resour., 46, 85-110, 10.1146/annurev-environ-012220-125406, 2021.

Laskar, A. H., Peethambaran, R., Adnew, G. A., and Röckmann, T.: Measurement of 18O18O and 17O18O in atmospheric O2 using the 253 Ultra mass spectrometer and applications to stratospheric and tropospheric air samples, Rapid Communications in Mass Spectrometry, 33, 981-994, https://doi.org/10.1002/rcm.8434, 2019

Leuenberger, M. C., Schibig, M. F., and Nyfeler, P.: Gas adsorption and desorption effects on cylinders and their importance for long-term gas records, Atmos. Meas. Tech., 8, 5289–5299, https://doi.org/10.5194/amt-8-5289-2015, 2015

Leuenberger, M., Nyfeler, P., Moret, H. P., Sturm, P., and Huber, Ch.: A new gas inlet system for an isotope ratio mass spectrometer improves reproducibility, Rapid Communications in Mass Spectrometry, 14, 1543–1551, https://doi.org/10.1002/1097-0231(20000830)14:16<1543::AID-RCM62>3.0.CO;2-H, 2000

Meija, J., Coplen, T. B., Berglund, M., Brand, W. A., De Bièvre, P., Gröning, M., Holden, N. E., Irrgeher, J., Loss, R. D., Walczyk, T., and Prohaska, T.: Isotopic compositions of the elements 2013 (IUPAC Technical Report), Pure and Applied Chemistry, 88, 293-306, https://doi.org/10.1515/pac-2015-0503, 2016